

Estimation of Radiated Fields of Small Horizontal Submodules Based on a Lumped-Element Model

Martin VÁLEK¹, Marco LEONE²

¹ Dept. of Electromagnetic Field, Czech Technical University, Technická 2, 166 27 Prague, Czech Republic

² Inst. für Grundlagen der Elektrotechnik und EMV, OvG-Universität Magdeburg, Universitätsplatz 2, 39016 Magdeburg, Germany

valek@siemens.com, marco.leone@e-technik.uni-magdeburg.de

Abstract. A novel approach to the estimation of radiated electric field of small horizontal submodules is presented. The principle idea is to describe the radiating submodule-on-motherboard structure with a lumped-element equivalent circuit which includes both the geometrical and the electrical parameters. The electromagnetic emission from the structure is approximated by the radiation characteristics of a Hertzian dipole driven by the antenna voltage resulting from the connector equivalent circuit. Therefore, no time consuming numerical field simulations are needed to evaluate the radiated electric field. Instead, a fast frequency circuit analysis with e.g. PSPICE is sufficient. Moreover, this modeling approach provides a clear insight concerning the influence of geometrical and electrical parameters with respect to radiated emissions. Finally, the computational solutions are compared with experimental results, demonstrating a good correspondence regarding engineering purposes.

Keywords

EMI of submodules, radiated emissions, lumped-element model, connector equivalent circuit, PSPICE analysis.

1. Introduction

The submodule-on-motherboard structure is a very popular solution to deal with limited space in the physical design of modern electronic equipment. However, a small potential difference between the reference planes of the motherboard and the subboard drives the submodule against the motherboard as a very short monopole antenna. The potential difference V_{ant} originates from the small but non-negligible signal-return impedance in the interboard connector provided by the ground pins. The radiation may reach relatively high levels when harmonics of a high-speed signal routed through the connector are close to the structure resonance frequency [1], [2]. Hence, a submodule introduces an efficient unintentional radiator of electromagnetic fields into the design of an electronic device. This

can lead to significant problems regarding the compliance to electromagnetic interference standards. A redesign of the device due to the non-conformance to EMC standards is very costly especially because of a design freeze in the testing phase before the serial production. This is the motivation for engineers to deal with this EMC issue at the early design stage of the submodule.

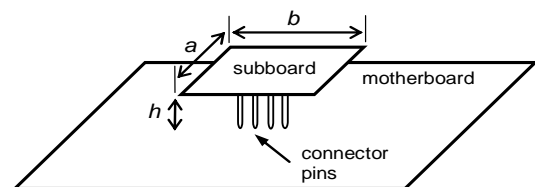


Fig. 1. The horizontal submodule on a motherboard (schematic).

The investigations presented in this paper focus on small horizontal submodule structures schematically illustrated in Fig. 1. The numerical field simulations of the horizontal submodule-on-motherboard structures have been already published in [3].

In contrast to [3], this paper introduces a novel approach to the radiated field estimation, based on a lumped-element equivalent circuit of the interboard connector from [2] extended with an antenna model. The driving antenna voltage V_{ant} can be computed by a fast frequency analysis of the lumped-element circuit and consequently applied to the antenna model. The main advantage of this approach is that only the commonly used circuit-analysis tools such as PSPICE are necessary to evaluate the electromagnetic interferences (EMI) instead of more time consuming and sophisticated field simulators.

2. Lumped-Element Model

The lumped-element model comprises the following parts:

- An equivalent circuit of the interboard connector
- An antenna model of a small horizontal submodule.

The physical characteristics of each part are described by means of lumped elements. The connector equivalent

circuit is indicated on the left side from V_{ant} in Fig. 2, while the antenna structure is defined by the electrical parameters R_{rad} and C_{ant} in Fig. 2.

The idea to separate the driving antenna voltage V_{ant} from the antenna structure was mentioned in [2] for the first time. However, the field simulations are still needed for the antenna transfer function in [2]. In this paper, the antenna transfer function is approximated by the electric far field of a Hertzian dipole [4].

To assign the correct lumped element to each of the physical characteristics of the submodule-on-motherboard structure further approximations are necessary, as shown in Fig. 1. The motherboard and the subboard are considered as perfectly conducting planes [1]. The connector pins may be simply represented by short wires [2], [3]. The wire length h corresponds to the height of the interboard connector.

According to the concept of partial inductances [4], a segment of a conductor embodies an external inductance which can be expressed by means of a self partial inductance. The external self partial inductance L_p of a thin wire dominates the internal wire inductance and it is frequency independent. The coupling between the pins is considered by mutual partial inductances M_n (Fig. 2).

The pins are assumed to be parallel to each other. Each new ground pin added into the connector introduces an additional partial self inductance L_p in parallel. The signal source is represented by the Thévenin equivalent, comprising the voltage generator V_s and the internal impedance of the source, which is lumped with the load impedance to the total signal impedance Z_t .

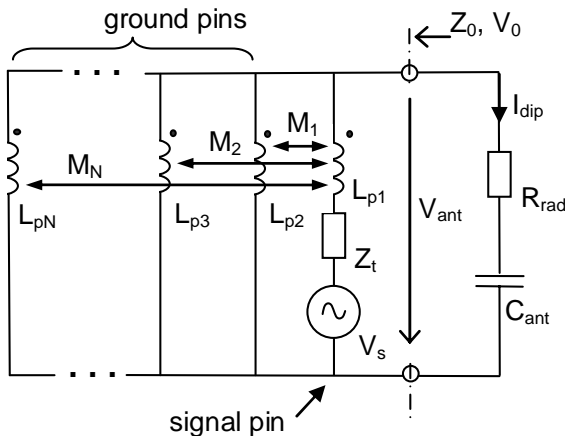


Fig. 2. The lumped-element model of small horizontal sub-modules.

2.1 Model of the Interboard Connector

The self partial inductance L_p of a pin with circular cross section can be computed from [4]

$$L_p = \frac{\mu_0}{2\pi} h \left[\ln \left(\frac{2h}{\rho} + \sqrt{\left(\frac{2h}{\rho} \right)^2 + 1} \right) + \frac{\rho}{2h} - \sqrt{\left(\frac{\rho}{2h} \right)^2 + 1} \right] \quad (1)$$

In terms of known physical dimensions: the pin radius ρ and the connector height h . Each pin is coupled with all neighboring pins by a mutual partial inductance M_n [2], [4]

$$M_n = \frac{\mu_0}{2\pi} h \left[\ln \left(\frac{2h}{n \cdot s} + \sqrt{\left(\frac{2h}{n \cdot s} \right)^2 + 1} \right) + \frac{n \cdot s}{2h} - \sqrt{\left(\frac{n \cdot s}{2h} \right)^2 + 1} \right] \quad (2)$$

where $n = 1, 2, 3 \dots N$ is an integer index and s is the uniform pin separation as given by the connector pitch. Expressions (1) and (2) differ from those published in [4] as the presence of the large motherboard reference plane is considered by the image principle [5]. The mutual coupling can be alternatively expressed by the coupling factor

$$K_n = \frac{M_n}{L_p} \quad (3)$$

The mutual inductance M_n decreases with increasing multiple distance $n \cdot s$. Thus, the following applies: $K_1 > K_2 > K_3 \dots > K_N$.

2.2 Antenna Model of a Small Horizontal Submodule

Assuming the dimensions of the submodule to be considerably smaller than the signal wavelength, the antenna impedance of the structure can be described by a lumped-element model comprising the capacitance C_{ant} and the radiation resistance R_{rad} . The subboard is usually much smaller than the motherboard. Hence, the parameter C_{ant} in Fig. 2 is well approximated by the capacitance of a metallic patch above an infinite ground plane. Because of the fringing effects, the effective area of the subboard is larger than the physical area. With reference to the $h/2$ rule [7] to account for the fringing fields, we obtain the formula

$$C_{ant} \approx \epsilon_0 \frac{(a + 2h)(b + 2h)}{h} \quad (4)$$

where a and b are the dimensions of the subboard.

As already observed in [3], the radiation pattern of a horizontal motherboard-on-subboard structure is virtually identical to the far field of a Hertzian monopole. This applies to the frequency region up to the first resonance of the structure. The structure radiation resistance R_{rad} is given by one half of the radiation resistance of a Hertzian dipole [4], according to the image principle

$$R_{rad} = \frac{1}{2} 80 \left(\frac{h}{c_0} \omega \right)^2 \quad (5)$$

where c_0 is the light velocity in vacuum in meters per second, h is the connector height in meters and ω is the frequency in radians per second. For a worst-case estimation, only the maximum magnitude of the electric field strength E_{max} in the far field is considered. Accounting for the ground plane on the motherboard by the factor of two (image principle), E_{max} of a Hertzian dipole [4] is

$$E_{max} = 2 \cdot \frac{\mu_0 \omega \cdot I_{dip} \cdot h}{4\pi r} \quad (6)$$

with the free-space permeability μ_0 and the observation distance r . Expressing the dipole current I_{dip} in terms of the antenna voltage V_{ant} (Fig. 2):

$$I_{dip} = \frac{\omega C_{ant} V_{ant}}{\sqrt{(\omega C_{ant} R_{rad})^2 + 1}} \approx \omega C_{ant} V_{ant} \quad (7)$$

we alternatively obtain

$$E_{max} = \frac{\mu_0 \omega^2 C_{ant} V_{ant} h}{2\pi r} \quad (8)$$

The frequency response of V_{ant} is obtained as result of simulation of the equivalent circuit in Fig. 2.

3. Resonance Frequency

The magnitude of the antenna voltage V_{ant} and the resonance frequency of the lumped-element model are the most relevant parameters for further EMC analysis. The magnitude of V_{ant} determines the radiated electric-field level E_{max} , according to (8). The resonance frequency ω_{res} defines the peak in the frequency response of E_{max} . The antenna voltage V_{ant} from the equivalent model of the sub-board-on-motherboard structure (Fig. 2) can be computed with a customary circuit-simulation tool such as PSPICE. However, the value of the parameter R_{rad} must be found beforehand. This requires an estimation of the resonance frequency ω_{res} . The suggestion how to roughly estimate ω_{res} has been done in [6]. The resonance issue is in more detail discussed in the subsection 3.1.

3.1 Basic Investigations

The impedance conditions in the model of Fig. 2 can be summarized by the equivalent circuit shown in Fig. 3. The interboard connector model with its pin inductances L_{pn} in parallel, mutual inductances M_n as well as the generator voltage V_s and the total signal impedance Z_t are transformed to Z_0 and V_0 . The capacitance C_{ant} and the radiation resistance of the antenna model are lumped to the parameter Z_{ant} . The magnitude of Z_{ant} decreases at -20 dB/decade which is typical for a capacitive impedance [5], while the magnitude of Z_0 has an inductive character with the typical increase of 20 dB/decade [5].

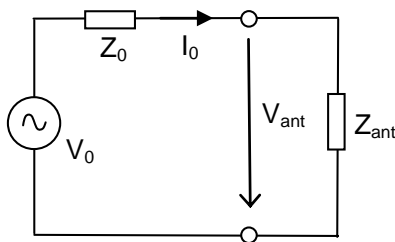


Fig. 3. General representation of the lumped-element model.

The series combination of Z_0 and Z_{ant} exhibits a minimum at the resonance frequency ω_{res} as the asymptotic impedance characteristics in Fig. 4 demonstrates.

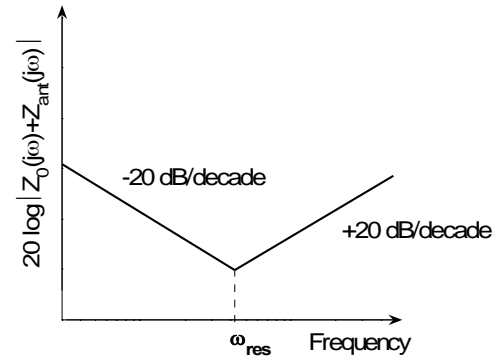


Fig. 4. An asymptotic impedance characteristics of the general representation of the lumped-element model.

To illustrate the case, a simple passive interboard connector has been analyzed. This is the case of a connector with one signal and one ground pin. Therefore, the connector model of Fig. 2 includes only L_{p1} , L_{p2} , M , Z_t and V_s . Considering $L_{p1} = L_{p2} = L_p$ and $M_1 = M$, we obtain the connector model shown in Fig. 5. Hence, the voltage V_0 is

$$V_0 = V_s \frac{j\omega(\Delta L)}{Z_t + 2j\omega(\Delta L)} \quad (9)$$

where $\Delta L = L_p - M$. Then, Z_0 is expressed as

$$Z_0 = \frac{j\omega L_p (Z_t + j\omega \Delta L) - \omega^2 \Delta L M}{Z_t + 2j\omega \Delta L} \quad (10)$$

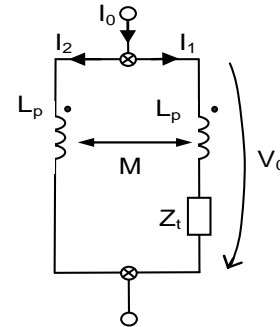


Fig. 5. Connector model with one signal and one ground pin for the calculation of Z_0 .

Since R_{rad} can be neglected, the antenna impedance is

$$Z_{ant} = \frac{1}{j\omega C_{ant}} \quad (11)$$

From the general representation of the lumped-element model in Fig. 3, the driving antenna voltage V_{ant} equals

$$V_{ant} = \frac{V_0}{1 + Z_0 / Z_{ant}} \quad (12)$$

The combination of (16) and (9) leads to the following transfer function

$$\frac{V_{ant}}{V_s} = \frac{j\omega\Delta L}{(Z_t + 2j\omega\Delta L)(1 + Z_0/Z_{ant})}. \quad (13)$$

Substituting Z_0 from (10) and Z_{ant} from (11)

$$\frac{V_{ant}}{V_s} = \frac{j\omega\Delta L}{Z_t \left[1 - \left(\frac{\omega}{\omega_1} \right)^2 \right] + 2j\omega\Delta L \left[1 - \left(\frac{\omega}{\omega_2} \right)^2 \right]} \quad (14)$$

where

$$\omega_1 = \frac{1}{\sqrt{L_p C_{ant}}}, \quad (15)$$

$$\omega_2 = \frac{1}{\sqrt{\frac{L_p + M}{2} C_{ant}}}. \quad (16)$$

Equations (15) and (16) identify the two limiting values for the resonance frequency ω_{res} of the transfer function (13). The actual ω_{res} lies within the closed interval $\langle \omega_1; \omega_2 \rangle$. The situation is illustrated in Fig. 6 for the parameters L_p , M and C_{ant} computed from the expressions (1), (2) and (4) and geometrical dimensions according to Tab. 1. A usual value of $Z_t = 50 \Omega$ has been considered for the total signal impedance Z_t . The width of the resonance interval is given by the relation

$$\frac{\omega_1}{\omega_2} = \sqrt{\frac{1}{2}(1 + K)}. \quad (17)$$

The coupling factor K has values within the open interval (0; 1). Hence, ω_1 is the lower and ω_2 is the upper limit resonance frequency.

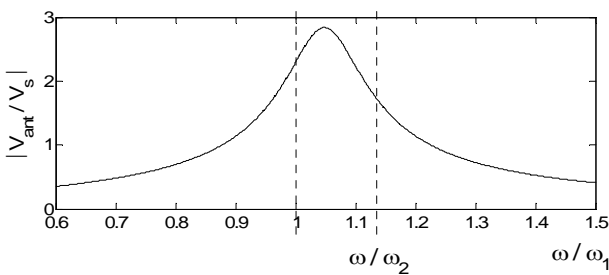


Fig. 6. The lower and the upper limits for the resonance frequency ω_{res} .

Motherboard	230 mm x 220 mm
Subboard	b = 70 mm, a = 50 mm
Connector	h = 15 mm, s = 2.5 mm, rho = 0.4 mm

Tab. 1. Dimensions of the submodul-on-motherboard structure for the computational examples.

3.2 Estimation of the Resonance Frequency

The expressions (15) and (16) differ only by the inductance values, corresponding to the two limiting cases of the total pin inductance L_{tot} , depending on the value of Z_t . The total pin inductance L_{tot} of the connector according to the equivalent circuit in Fig. 5 varies between the value of L_p in the case of $|Z_t| \gg \omega(L_p + M)$ and the value of $(L_p + M)/2$ in the case of $|Z_t| \ll \omega(L_p + M)$. Hence, the expressions (15) and (16) can be rewritten as

$$\omega_1 = \frac{1}{\sqrt{L_{tot}^{(N-1)} C_{ant}}}, \quad (18)$$

$$\omega_2 = \frac{1}{\sqrt{L_{tot}^{(N)} C_{ant}}}, \quad (19)$$

where N is the number of all pins. Equations (18) and (19) can be applied for an arbitrary number of all connector pins with the following approximations, in order to enable the derivation of a simple closed-form expression.

- All connector pins have the same self partial inductance L_p (the same geometry).
- Only the contribution M_1 from the closest neighboring pins is considered, as shown in Fig. 7.

The actual occurrence of the resonance within the interval $\langle \omega_1; \omega_2 \rangle$ is strongly dependent on the relationship between $|Z_t|$ and $\omega(L_p + M)$. However, the resonance frequency ω_{res} appears close to the middle of the interval for the common values of Z_t , L_p and M .

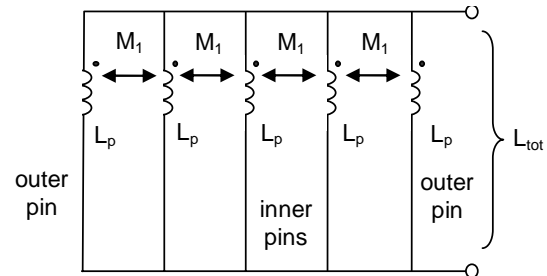


Fig. 7. Simplified coupling model of the connector.

For the modeling approach introduced in this paper, the arithmetic mean value of ω_1 and ω_2 is an acceptable approximation for ω_{res} . Thereby, the resonance of the lumped-element model can be described with an approximative formula

$$\omega_{res} \approx \frac{1}{\sqrt{L_{tot} C_{ant}}} \quad (20)$$

where

$$L_{tot} \approx \frac{1}{2} (L_{tot}^{(N-1)} + L_{tot}^{(N)}). \quad (21)$$

The total pin inductance L_{tot} in the case of the simplest connector configuration with one signal and only one ground pin ($N_G = 1$) is

$$L_{tot} \approx L_p \frac{1}{2} \left(1 + \frac{1+K_1}{2} \right). \quad (22)$$

The total pin inductance for the interboard connectors with more than one ground pin ($N_G > 1$) can be approximated by the following formula [6]

$$L_{tot} \approx L_p \frac{1+K_1}{4} \left(\frac{1}{1 + \frac{(N_G - 2)(1+K_1)}{2(1+2K_1)}} + \frac{1}{1 + \frac{(N_G - 1)(1+K_1)}{2(1+2K_1)}} \right). \quad (23)$$

4. Computational Examples

The approach to the estimation of the electric field radiated from small horizontal submodules is demonstrated by two computational examples, referring to the numerical results of full-wave simulations. The geometrical parameters of the submodule-on-motherboard structure used in the computational examples are given in Tab. 1.

The first example represents the simplest case of an interboard connector configuration with one signal and one ground pin. The corresponding PSPICE circuit of the structure is shown in Fig. 8, with the following parameters calculated from the expressions (1) to (4): $L_{p1} = L_{p2} = 12$ nH, $M_I = 6.8$ nH, $K_1 = 0.562$, $C_{ant} = 4.72$ pF. The value of the radiation resistance R_{rad} was estimated equal to 2.0Ω according to (20). The amplitude of the signal-source V_s and the total signal impedance Z_t from the lumped-element model of Fig. 2 have been chosen 1 Volt and 50Ω , respectively. Despite the relatively small value of R_{rad} , the inclusion of the radiation resistance was found to be necessary, in order to avoid greater errors in the computation of the resonance amplitude.

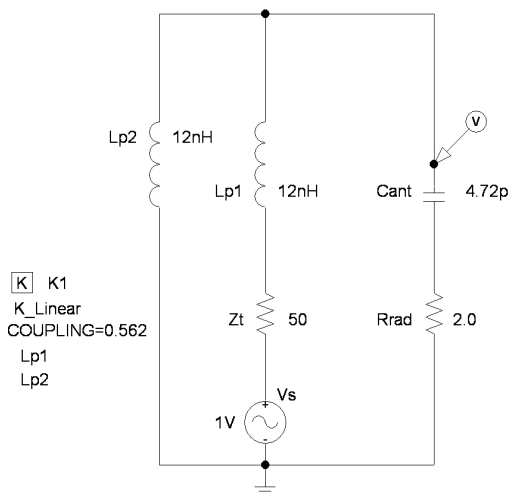


Fig. 8. PSPICE model of the subboard-on-motherboard structure with a connector containing one signal and one ground pin.

The frequency response of the antenna voltage V_{ant} across the capacitor C_{ant} was computed by PSPICE and used for the subsequent calculation of the maximum radiated electric field E_{max} as given by the equation (8).

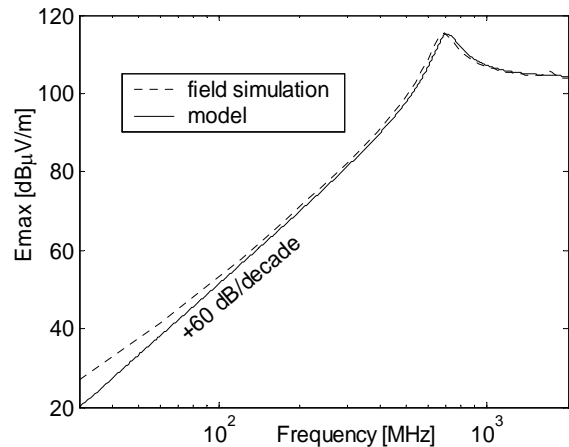


Fig. 9. Maximum electric field strength at 1 m distance for a connector with one signal and one ground pin.

Fig. 9 shows the resulting frequency response of E_{max} at the distance $r = 1$ m from the structure. As a reference, also the results of a full-wave field simulation (MoM [8]) are included. A very good correspondence of the presented model is observed.

In the next example, the same geometrical parameters as in the previous example are considered. However, in this case, the interboard connector includes four ground pins instead of one. The connector equivalent model is extended by the additional three self inductances $L_{p3} = L_{p4} = L_{p5} = 12$ nH in parallel to L_{p2} and the corresponding mutual inductances (Fig. 2). The radiation resistance increases to $R_{rad} = 4.3 \Omega$ due to the higher resonance frequency of the structure as a consequence of the lower total inductance L_{tot} . Additional coupling factors K must be included: $K_2 = 0.41$, $K_3 = 0.33$ and $K_4 = 0.2$. The results of our model and the field simulation are shown in Fig. 10. Also in this case, the results of the modeling approach match quite well to the field-simulation results.

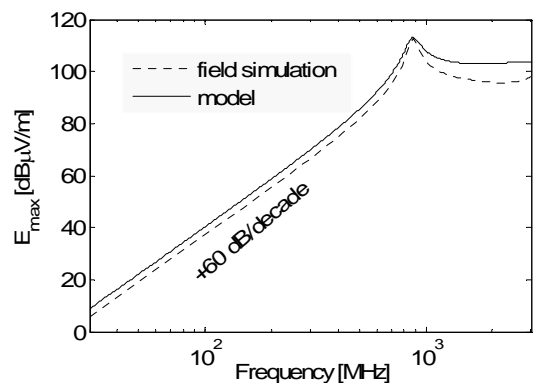


Fig. 10. Maximum electric field strength in the far field at 1 m distance for a connector with one signal and 4 ground pins.

5. Experimental Validation

As a further validation of the presented modeling approach, a measurement was performed in a 3 m semi-anechoic chamber. For this purpose, a test-board structure was constructed [3], [6] with identical physical dimensions as given in the computational examples (Fig. 11).

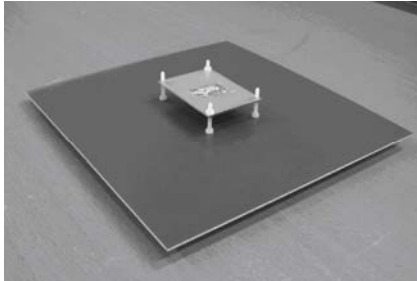


Fig. 11. Test-board structure for experimental validation of the suggested radiation model.

The emission measurement was performed with an EMI receiver (Rohde&Schwarz ESVS 30). The structure was fed through an SMA connector by the harmonic signal of the tracking generator (output power 0 dBm). An attenuator of 20 dB was used to reduce reflections on the feeding cable due to the impedance mismatch between the generator output and the interboard connector input. In the simulations the signal amplitude of the voltage generator V_s was set to 22.3 mV corresponding to the power of -20dBm on the total signal impedance $Z_t = 50 \Omega$. In the equivalent model and in the field simulation, an additional inductance of 10 nH was added in series to the signal pin to account for the influence of the SMA connector. The value of the connector inductance was empirically determined from an S-parameter measurement.

Fig. 12 shows the comparison of the measurement results (solid line) with the results of the modeling approach (dotted line) and the field simulation (dash-dot line). Below 300 MHz, the small radiation level is masked by the system noise. Considering a typical emission measurement uncertainty of around 1.5 dB as well as parameter tolerances of the test board, an acceptable correspondence is obtained.

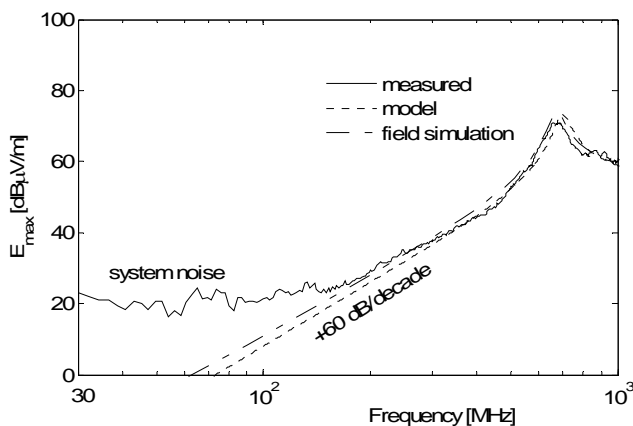


Fig. 12. Experimental validation of the suggested modeling approach.

6. Conclusion

A novel approach is presented to estimate the radiated emission of small horizontal submodule-on-motherboard structures. It is based on a lumped-element model which includes an equivalent circuit of the interboard connector and an antenna model of the structure. The main advantage of this modeling approach is the possibility to quickly estimate the radiated electric field just by a circuit analysis with no need for further numerical field simulations. The origin of the characteristic resonance of a horizontal submodule-on-motherboard structure has been found to be a series resonance of the connector total inductance and the capacitance of the submodule to the motherboard ground. Practical closed-form expressions for the estimation of the resonance frequency have been introduced. In contrast to a more time-consuming full-wave field simulation, the approach additionally provides a clear insight to the radiation mechanism and reveals how the individual geometrical and electrical parameters influence the radiation behavior. As shown by the comparison with 3D-field simulations as well as with measurements in a semi-anechoic chamber, the suggested model provides a sufficient accuracy for engineering purposes.

Acknowledgements

The research described in the paper was technically supported by the Dept. of EMC&Testing in the Center for Quality Engineering of Siemens Communications in Munich, Germany.

References

- [1] LI, K., TASSOUDI, A., POH, S. Y., TSUK, M., SHIN, R. T., KONG, J. A. FD-TD analysis of electromagnetic radiation from modules-on-backplane configurations. *IEEE Transactions on Electromagnetic Compatibility*. 1995, vol. 37, no 3, pp.326 – 332.
- [2] LEONE, M., NAVRÁTIL, V. On the electromagnetic radiation of printed-circuit-board interconnections. *IEEE Transactions on Electromagnetic Compatibility*. 2005, vol. 47, no. 2, pp.219 – 226.
- [3] VÁLEK, M., LEONE, M., SCHMIEDL, F. Analysis of the radiation behaviour of motherboard-subboard structures. In *Proc. of the 6th International Symposium on Electromagnetic Compatibility and Electromagnetic Ecology*. St.-Petersburg (Russia), 2005, pp.175-178.
- [4] PAUL, C. R. *Introduction to Electromagnetic Compatibility*. New York: John Wiley & Sons, Inc., 1992.
- [5] BALANIS, C. A. *Antenna Theory*. New York: John Wiley & Sons, Inc., 1997.
- [6] VÁLEK, M., LEONE, M. Radiation model for small horizontal submodules. In *Proceedings of the VII EMC Europe*. Barcelona (Spain), 2006, pp.426-430.
- [7] LANGE, K., LÖCHERER, K.-H. *Taschenbuch der Hochfrequenztechnik*. Springer-Verlag, 1986.
- [8] CONCEPT Home Page: www.tu-hamburg.de/~tebr

About Authors...

Martin VÁLEK was born in Prague, Czech Republic in August 1978. He received the M.Sc. degree in Radioelectronics from the Czech Technical University (CTU) in Prague in 2003. He worked as an EMC engineer for the automotive industry from 2003 to 2004. In 2004, he joined Siemens Communications to start with the research of the EMI from submodules in the Center of Quality Engineering in Munich, Germany. Since 2004, he has been a Ph.D. student with the Dept. of Electromagnetic Field at the CTU Prague. His research interests include development of novel methods for the EMC testing of submodules and EMC support for R&D engineers.

Marco LEONE was born in Zurich, Switzerland in 1966. He graduated in 1990 at the University of Applied Sciences Frankfurt am Main, Germany in Communications Engineering and received the Dipl. Ing. degree from the Technical University of Berlin, in 1995 in General and Theo-

retical Electrical Engineering. In 2000 he received the Dr. Ing. degree from the Technical University Hamburg-Hamburg, Germany, where he was a research and teaching assistant in the Department of Theoretical Electrical Engineering from 1996 to 2000. From 2000-2004 he was with the Siemens AG Corporate Technology Department in Erlangen, Germany, where he worked as Senior Engineer in the field of analytical and numerical modeling of radiation mechanisms on printed-circuit-board and system level. In 2004 he changed to the Siemens Communications in the Center of Quality Engineering in Munich, Germany, where he was the manager for printed-circuit board EMC projects. In 2006 he has been appointed as full professor at the Otto-von-Guericke-Universität of Magdeburg, Germany, where he holds the chair for Theoretical Electrical Engineering. Prof. Leone is the recipient of the Best Paper Awards of the EMV 2002, EMV 2004 and EMV 2006 International Symposium, Düsseldorf, Germany, and of the 2003 Best Paper Award of the IEEE International Symposium on EMC 2003, Boston, USA.

Call for Papers

Advanced Signal Processing

A Special Issue of

Radioengineering

October 15, 2007: Submission of a paper

A paper is requested being submitted via e-mail to editor@radioeng.cz. The manuscript has to be prepared in MS Word for Windows in Radioengineering Publishing Style. The example document with proper styles is available at:

<http://www.radioeng.cz>

Due to the very short publication time, extreme care has to be devoted to the formal processing of the paper. A paper of an inadequate form might be rejected from that reason. An author is encouraged to submit a PDF version of the paper together with the MS Word document in order to simplify handling the paper.

October 31, 2007: Notification of acceptance

Two independent reviewers review a paper submitted. Reviews are distributed to the authors via e-mail. If paper is accepted for publication, authors are asked to revise the paper in accordance with review comments.

November 15, 2007: Submission of a revised paper

The revised paper has to be delivered to the editors via e-mail in the form of the MS Word document as described in "Submission of a paper".